Albumin-Binding and Conventional PSMA Ligands in Combination with ^{161}Tb: Biodistribution, Dosimetry, and Preclinical Therapy

Viviane J. Tschan*[1], Sarah D. Busslinger*[1], Peter Bernhardt[2], Pascal V. Grundler[1], Jan Rijn Zeevaart[3], Ulli Köster[4], Nicholas P. van der Meulen[1,5], Roger Schibli[1,6], and Cristina Müller[1,6]

[1]Center for Radiopharmaceutical Sciences ETH–PSI, Paul Scherrer Institute, Villigen-PSI, Switzerland; [2]Department of Radiation Physics, Institution of Clinical Science, Sahlgrenska Academy, University of Gothenburg, Gothenburg, Sweden; [3]Radiochemistry, South African Nuclear Energy Corporation (Necsa), Brits, South Africa; [4]Institut Laue-Langevin, Grenoble, France; [5]Laboratory of Radiochemistry, Paul Scherrer Institute, Villigen-PSI, Switzerland; and [6]Department of Chemistry and Applied Biosciences, ETH Zurich, Zurich, Switzerland

The favorable decay characteristics of ^{161}Tb attracted the interest of clinicians in using this novel radionuclide for radioligand therapy (RLT). ^{161}Tb decays with a similar half-life to ^{177}Lu, but beyond the emission of β^--particles and γ-rays, ^{161}Tb also emits conversion and Auger electrons, which may be particularly effective to eliminate micrometastases. The aim of this study was to compare the dosimetry and therapeutic efficacy of ^{161}Tb and ^{177}Lu in tumor-bearing mice using SibuDAB and PSMA-I&T, which differ in their blood residence time and tumor uptake. **Methods:** [^{161}Tb]Tb-SibuDAB and [^{161}Tb]Tb-PSMA-I&T were evaluated in vitro and investigated in biodistribution, imaging, and therapy studies using PC-3 PIP tumor–bearing mice. The ^{177}Lu-labeled counterparts served for dose calculations and comparison of therapeutic efficacy. The tolerability of RLT in mice was monitored on the basis of body mass, blood plasma parameters, blood cell counts, and the histology of relevant organs and tissues. **Results:** The prostate-specific membrane antigen (PSMA)–targeting radioligands, irrespective of whether labeled with ^{161}Tb or ^{177}Lu, showed similar in vitro data and comparable tissue distribution profiles. As a result of the albumin-binding properties, [^{161}Tb]Tb/[^{177}Lu]Lu-SibuDAB had an enhanced blood residence time and higher tumor uptake (62%–69% injected activity per gram at 24 h after injection) than [^{161}Tb]Tb/[^{177}Lu]Lu-PSMA-I&T (30%–35% injected activity per gram at 24 h after injection). [^{161}Tb]Tb-SibuDAB inhibited tumor growth more effectively than [^{161}Tb]Tb-PSMA-I&T, as can be ascribed to its 4-fold increased absorbed tumor dose. At any of the applied activities, the ^{161}Tb-based radioligands were therapeutically more effective than their ^{177}Lu-labeled counterparts, as agreed with the approximately 40% increased tumor dose of ^{161}Tb compared with that of ^{177}Lu. Under the given experimental conditions, no obvious adverse events were observed. **Conclusion:** The data of this study indicate the promising potential of ^{161}Tb in combination with SibuDAB for RLT of prostate cancer. Future clinical studies using ^{161}Tb-based RLT will shed light on a potential clinical benefit of ^{161}Tb over ^{177}Lu.

Key Words: PSMA; prostate cancer; ^{161}Tb; albumin-binding radioligand; radioligand therapy

J Nucl Med 2023; 64:1625–1631
DOI: 10.2967/jnumed.123.265524

Radioligand therapy (RLT) using prostate-specific membrane antigen (PSMA)–targeting radioligands emerged as an effective means for the treatment of patients with metastatic castration-resistant prostate cancer (*1–3*). The positive outcome of a clinical phase III study (VISION; NCT0351166) using [^{177}Lu]Lu-PSMA-617 (*4*) led to the approval of this radioligand (Pluvicto; Novartis) for the treatment of patients with PSMA-positive metastatic castration-resistant prostate cancer. [^{177}Lu]Lu-PSMA-I&T, a similar radioligand, has also been used clinically for the treatment of metastatic castration-resistant prostate cancer (*5–7*).

Currently, several clinical trials are ongoing to investigate a potential benefit of ^{177}Lu-based RLT in patients at an earlier disease stage (*8–12*). β^--particles have a relatively long tissue range (^{177}Lu, 2 mm) and thus are suitable for the treatment of macrometastases; however, they are not effective enough to eliminate micrometastases, an ability that would be essential for these patients to achieve long-term disease control. RLT using an α-particle emitter may be an option to address this situation; however, severe side effects will prevent the use of ^{225}Ac-based RLT in patients with a generally good prognosis (*13,14*).

^{161}Tb has attracted the attention of clinicians and researchers alike. It shares similar chemical properties and physical decay characteristics (β^--particles and γ-ray emission) with ^{177}Lu but coemits low-energy conversion and Auger electrons. Since Auger electrons have an ultrashort tissue range (<500 nm) and, hence, a high linear energy transfer (4–26 keV/μm), they may be particularly effective to eliminate single and clustered cancer cells (*15,16*). In our previous work, we demonstrated that ^{161}Tb outperforms ^{177}Lu in cell-based in vitro assays irrespective of the applied targeting concept (*17–19*). Preclinical therapy studies using [^{161}Tb]Tb-PSMA-617 in xenografted mice showed a dose-dependent tumor growth delay and survival.

Currently, [^{161}Tb]Tb-PSMA-I&T (VIOLET; NCT05521412 (*20*)) and [^{161}Tb]Tb-PSMA-617 (REALITY; NCT04833517 (*21*) are applied to metastatic castration-resistant prostate cancer patients in phase I and II clinical studies and on a compassionate-use basis under the local regulatory framework (*22*).

At the Paul Scherrer Institute, we have developed several generations of albumin-binding PSMA ligands that are characterized by an enhanced blood circulation time and, as a result, higher tumor accumulation than for PSMA-617 or PSMA-I&T.

Received Jan. 28, 2023; revision accepted May 31, 2023.
For correspondence or reprints, contact Cristina Müller (cristina.mueller@psi.ch).
*Contributed equally to this work.
Published online Jul. 13, 2023.

[^{177}Lu]Lu-PSMA-ALB-56, derivatized with a *p*-tolyl–based albumin binder, showed promising therapeutic efficacy in preclinical studies (*23*); however, the long blood residence time observed in patients affected the bone marrow dose unfavorably (*24*). [^{177}Lu]Lu-SibuDAB, the *S*-isomer of [^{177}Lu]Lu-Ibu-DAB-PSMA (*25,26*), was developed as an optimized PSMA ligand with moderate albumin-binding properties (*27*). The tolerability of this new class of ibuprofen-derivatized PSMA radioligands was in the same range as for conventional PSMA radioligands (*26*).

The goal of this study was to investigate SibuDAB in combination with ^{161}Tb and assess the potential benefit of this novel RLT concept. We performed preclinical studies to evaluate [^{161}Tb]Tb-SibuDAB and [^{161}Tb]Tb-PSMA-I&T in comparison to their ^{177}Lu-labeled counterparts with regard to dosimetry estimations and therapeutic efficacy.

MATERIALS AND METHODS

Detailed methods are presented as a supplemental data file (supplemental materials are available at http://jnm.snmjournals.org). This study was performed in agreement with national laws and the institutional internal guidelines on radiation safety.

Radioligand Preparation and In Vitro Characterization

SibuDAB (*S*-isomer of Ibu-DAB-PSMA (*27*)) and PSMA-I&T were labeled under standard conditions at molar activities of up to 50 MBq/nmol, with radiochemical purity of more than 98% (Supplemental Figs. 1 and 2). The radiolytic stability of [^{161}Tb]Tb-SibuDAB and [^{161}Tb]Tb/[^{177}Lu]Lu-PSMA-I&T, their distribution coefficients (logD values), and cell uptake in PSMA-positive PC-3 PIP and PSMA-negative PC-3 flu tumor cells (provided by Martin Pomper, Johns Hopkins University School of Medicine) were determined as previously reported for [^{177}Lu]Lu-SibuDAB (*27*). The in vitro albumin-binding capacity of the radioligands was determined according to an established protocol (*28*).

In Vivo Studies

All applicable international, national, or institutional guidelines for the care and use of laboratory animals were followed, and all animal experiments were performed according to the guidelines of Swiss Regulations for Animal Welfare. The preclinical studies were ethically approved by the Cantonal Committee of Animal Experimentation and permitted by the responsible cantonal authorities (license 75668).

Blood Clearance

The blood clearance of [^{161}Tb]Tb-SibuDAB (25 MBq, 1 nmol per mouse) was determined as previously reported for [^{177}Lu]Lu-SibuDAB using an immunocompetent mouse strain (FVB, Friend leukemia virus B) (*27*). The collected blood samples were measured to calculate the percentage injected activity (%IA) retained in the blood over 24 h, with the activity at t = 0 set as 100%.

Biodistribution Studies and Dosimetry Estimation

PC-3 PIP/flu tumor–bearing nude mice (BALB/c nude, Bagg Albino) were intravenously injected with the respective radioligand (5 MBq, 1 nmol per mouse). Tissues were collected, weighed, and counted for activity using a γ-counter. The decay-corrected results were listed as %IA per gram of tissue mass (%IA/g).

Dosimetry estimations were performed for tumors (assuming a sphere of 80 mm^3) and kidneys on the basis of the time-integrated activity concentration using non–decay-corrected biodistribution data for the ^{177}Lu-labeled PSMA ligands. The Monte Carlo code PENELOPE (penetration and energy loss of positrons and electrons) was used for determination of the energy deposits in the tissues (*29*).

Dual-Isotope SPECT/CT Imaging

Dual-isotope SPECT/CT was performed according to a previously established protocol using a small-animal SPECT/CT scanner (*27*). PC-3 PIP/flu tumor–bearing BALB/c nude mice were injected with a mixture of [^{161}Tb]Tb-SibuDAB and [^{177}Lu]Lu-SibuDAB or [^{161}Tb]Tb-PSMA-I&T and [^{177}Lu]Lu-PSMA-I&T (20 MBq, 1 nmol per mouse in total). The images were reconstructed on the basis of γ-lines of ^{161}Tb or ^{177}Lu or the combined γ-lines.

Therapy Study

PC-3 PIP tumor–bearing BALB/c nude mice were treated with either [^{161}Tb]Tb-SibuDAB or [^{177}Lu]Lu-SibuDAB (2, 5, or 10 MBq, 1 nmol per mouse) or with [^{161}Tb]Tb-PSMA-I&T or [^{177}Lu]Lu-PSMA-I&T (5 or 10 MBq, 1 nmol per mouse). Control mice received only vehicle (saline with 0.05% bovine serum albumin) (Supplemental Table 1). The body mass and tumor volume of the mice were monitored (*27*). The area under the curve of the relative tumor volume (AUC_{RTV}) for each mouse in a group was calculated and expressed as the average value per group. The median survival of mice was determined as a measure of the radioligands' therapeutic efficacy. Potential adverse events were determined on the basis of body mass, plasma parameters, blood cell counts, and analysis of histologic changes using a predefined scoring system (Supplemental Table 2).

Analysis and Statistical Methods

GraphPad Prism software (version 8) was used for data analysis, including determination of statistical significance ($P < 0.05$) and preparation of graphs.

RESULTS

In Vitro Characterization of Radioligands

The radioligands (25 MBq/nmol) were stable over 4 h in saline at room temperature (>95% of intact radioligand). The logD values of [^{161}Tb]Tb-SibuDAB (−2.5 ± 0.1) and [^{161}Tb]Tb-PSMA-I&T (<−4) were similar to those of [^{177}Lu]Lu-SibuDAB (−2.3 ± 0.1 (*27*)) and [^{177}Lu]Lu-PSMA-I&T (<−4), respectively.

PC-3 PIP tumor cell uptake and internalization of [^{161}Tb]Tb-SibuDAB (54% ± 1% and 18% ± 2%, respectively) and [^{161}Tb]Tb-PSMA-I&T (42% ± 6% and 11% ± 2%, respectively) were in the same range as for their respective ^{177}Lu-labeled counterparts (Fig. 1A). Negligible uptake of the radioligands (<1%) was observed in PC-3 flu cells.

The protein-bound fraction of [^{161}Tb]Tb-SibuDAB and [^{177}Lu]Lu-SibuDAB (*28*) was approximately 90% in undiluted mouse and human blood plasma (Figs. 1B and 1C) but much lower for [^{161}Tb]Tb-PSMA-I&T and [^{177}Lu]Lu-PSMA-I&T (50%–60%) (Figs. 1B and 1C). Affinity curves determined using variable serum albumin-to-radioligand molar ratios confirmed the strong plasma protein binding of SibuDAB as compared with only moderate binding of PSMA-I&T irrespective of the used radionuclide in both mouse and human plasma (Figs. 1B and 1C).

Blood Clearance and Biodistribution Data

Equal blood clearance curves were obtained for [^{161}Tb]Tb-SibuDAB as previously determined for [^{177}Lu]Lu-SibuDAB (*27*) in immunocompetent mice without tumors ($P > 0.05$; Fig. 2A).

The blood retention of [^{161}Tb]Tb-SibuDAB in tumor-bearing BALB/c nude mice (6.5 ± 3.7 %IA/g and 0.32 ± 0.05 %IA/g at 4 and 24 h after injection, respectively) was considerably enhanced as compared with that of [^{161}Tb]Tb-PSMA-I&T (<0.1%IA/g at 4 h after injection). As a result, the tumor uptake of [^{161}Tb]Tb-SibuDAB was almost twice as high (75 ± 5 %IA/g) as for [^{161}Tb]Tb-PSMA-I&T

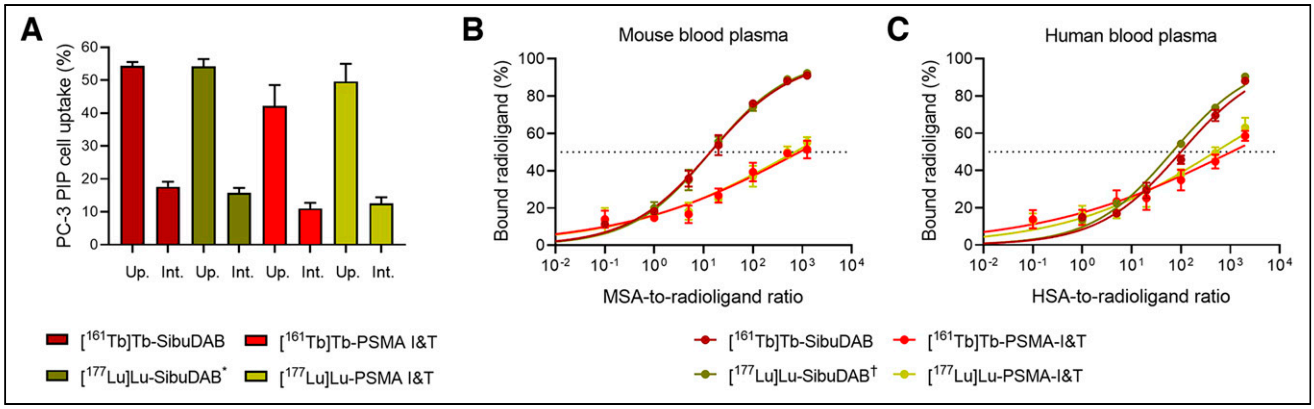

FIGURE 1. (A) Cell uptake and internalization of [^{161}Tb]Tb/[^{177}Lu]Lu-SibuDAB and [^{161}Tb]Tb/[^{177}Lu]Lu-PSMA-I&T in PC-3 PIP cells after 4 h of incubation (average ± SD). (B and C) In vitro albumin-binding curves of [^{161}Tb]Tb/[^{177}Lu]Lu-SibuDAB and [^{161}Tb]Tb/[^{177}Lu]Lu-PSMA-I&T in mouse (B) and human (C) blood plasma. Dashed line indicates half-maximum (i.e., 50%) binding. HSA = human serum albumin; Int. = internalization; MSA = mouse serum albumin; Up. = uptake. *Data were previously published (*27*). †Data were previously published (*28*).

(42 ± 14 %IA/g) at 4 h after injection (Fig. 2B; Supplemental Tables 3 and 4). Kidney retention of [^{161}Tb]Tb-SibuDAB (16 ± 1 %IA/g) was in a similar range to that for [^{161}Tb]Tb-PSMA-I&T (18 ± 3 %IA/g) at this same time point. At the 24-h time point, less than 7 %IA/g was retained in the kidneys for both radioligands. Uptake in the tumors and kidneys at 4 and 24 h after injection of the ^{161}Tb-based PSMA ligands did not significantly differ from that for the ^{177}Lu-based counterparts ($P > 0.05$; Supplemental Tables 3 and 4). At 4 h after injection of any of the radioligands, activity retention was already less than 2% in nontargeted tissues such as the liver, spleen, and bone (Fig. 2B).

Dual-Isotope SPECT Imaging Studies

The SPECT images reconstructed on the basis of the γ-lines of ^{161}Tb or ^{177}Lu showed equal distribution in the blood, tumor, and kidneys of the same mouse, irrespective of the used radionuclide (Fig. 3). At 1 h after injection of [^{161}Tb]Tb-SibuDAB/[^{177}Lu]Lu-SibuDAB, blood retention was increased as compared with that of [^{161}Tb]Tb-PSMA-I&T/[^{177}Lu]Lu-PSMA-I&T, whereas kidney retention appeared somewhat lower for the former. At the 4-h time point, the differences between radiolabeled SibuDAB and PSMA-I&T were less pronounced (Fig. 3).

Dosimetry Estimations

Dosimetry data were calculated using extended biodistribution data acquired with the ^{177}Lu-based radioligands (Supplemental Tables 5 and 6), assuming equal distribution profiles for the ^{161}Tb- and ^{177}Lu-labeled counterparts (Figs. 2A and 3; Supplemental Tables 3 and 4). The mean absorbed PC-3 PIP tumor dose of [^{161}Tb]Tb-SibuDAB (10.8 ± 1.6 Gy/MBq) was about 40% higher than for [^{177}Lu]Lu-SibuDAB (7.7 ± 1.1 Gy/MBq), and the same held true for [^{161}Tb]Tb-PSMA-I&T (2.9 ± 0.3 Gy/MBq) as compared with [^{177}Lu]Lu-PSMA-I&T (2.1 ± 0.2 Gy/MBq). The mean absorbed kidney dose was 0.44 ± 0.04 Gy/MBq and 0.59 ± 0.04 Gy/MBq for the respective ^{161}Tb-labeled ligands and 0.32 ± 0.03 Gy/MBq and 0.43 ± 0.03 Gy/MBq for the ^{177}Lu-labeled counterparts. [^{161}Tb]Tb/[^{177}Lu]Lu-SibuDAB demonstrated an approximately 5-fold higher tumor-to-kidney dose ratio (~24.5) than [^{161}Tb]Tb/[^{177}Lu]Lu-PSMA-I&T (~4.8) (Supplemental Table 7).

Therapeutic Efficacy of Radioligands

In control mice, the tumors grew rapidly over time, with all mice reaching a predefined endpoint between days 14 and 28 (median survival, 18 d). ^{161}Tb-labeled PSMA ligands were consistently more effective at delaying tumor growth than the respective ^{177}Lu-labeled counterparts, irrespective of whether SibuDAB or PSMA-I&T was used (Fig. 4; Table 1). The increased therapeutic efficacy of [^{161}Tb]Tb-SibuDAB over [^{177}Lu]Lu-SibuDAB was most visible in mice that received 2 MBq, as demonstrated by a median survival of 32.5 versus 23 d, respectively. All mice treated with 5 MBq of [^{161}Tb]Tb-SibuDAB survived until study end, whereas 1 of 6 mice treated with 5 MBq [^{177}Lu]Lu-SibuDAB reached an endpoint on day 49. Treatment of the mice with 10 MBq of [^{161}Tb]Tb-SibuDAB resulted in complete tumor regression over the 2-mo observation period, whereas tumor regrowth was observed in 1 case approximately 6 wk after treatment with 10 MBq of [^{177}Lu]Lu-SibuDAB (Figs. 4A and 4C).

When the application was 5 MBq per mouse, 3 of 6 mice treated with [^{161}Tb]Tb-PSMA-I&T were alive at study end (median

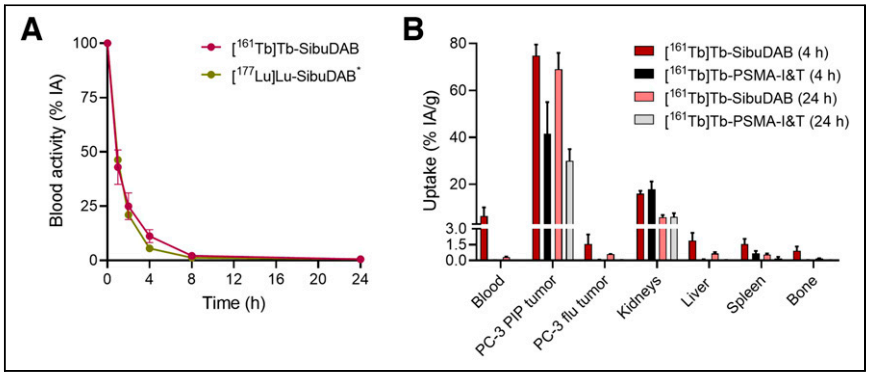

FIGURE 2. (A) Blood clearance of [^{161}Tb]Tb-SibuDAB and [^{177}Lu]Lu-SibuDAB over 24 h after injection. (B) Decay-corrected biodistribution data 4 and 24 h after injection of [^{161}Tb]Tb-SibuDAB and [^{161}Tb]Tb-PSMA-I&T. PC-3 flu = PSMA-negative tumor xenografts; PC-3 PIP = PSMA-positive tumor xenograft. *Data were previously published (*27*).

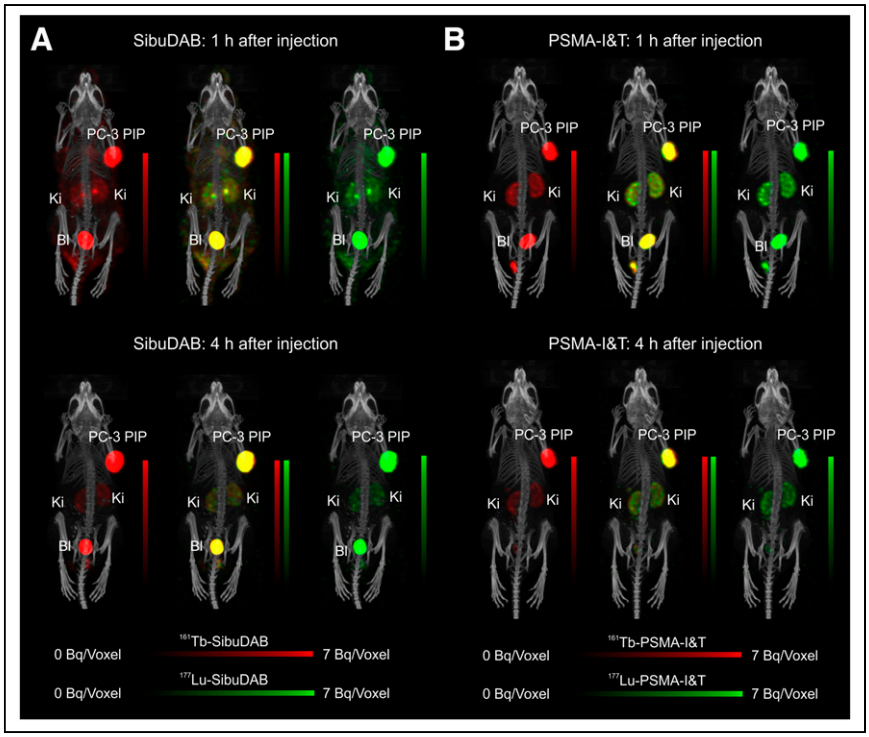

FIGURE 3. Dual-isotope SPECT/CT images of mice bearing PC-3 PIP (right shoulder) and PC-3 flu (left shoulder) tumor xenografts 1 and 4 h after injection of 1:1 mixture (20 MBq per mouse) of [^{161}Tb]Tb-SibuDAB and [^{177}Lu]Lu-SibuDAB (A) or [^{161}Tb]Tb-PSMA-I&T and [^{177}Lu]Lu-PSMA-I&T (B). Image reconstruction was based on γ-lines of ^{161}Tb (red), ^{177}Lu (green), or both (red/green overlay). Bl = bladder; Ki = kidneys; PC-3 flu = PSMA-negative tumor xenograft; PC-3 PIP = PSMA-positive tumor xenograft.

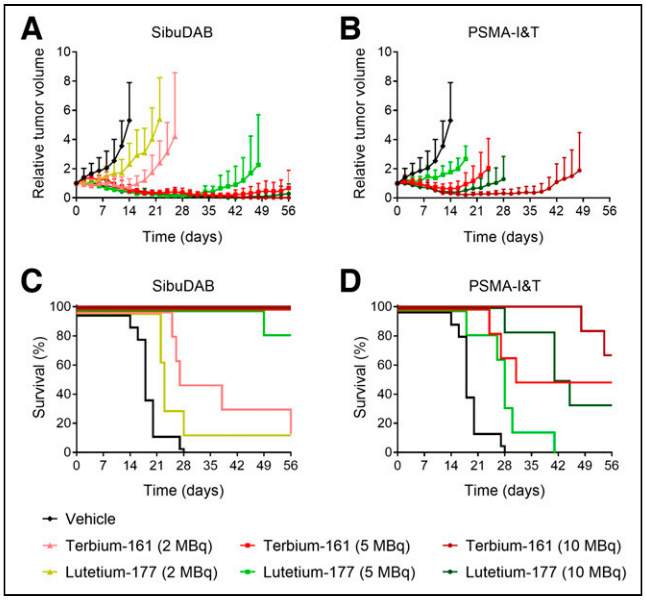

FIGURE 4. (A and B) Relative tumor growth curves shown until first mouse of respective group reached endpoint. (C and D) Kaplan–Meier plot (vertical offset was applied to improve readability). Mice received vehicle or were treated with [^{161}Tb]Tb-SibuDAB or [^{177}Lu]Lu-SibuDAB (A and C) or with [^{161}Tb]Tb-PSMA-I&T or [^{177}Lu]Lu-PSMA-I&T (B and D). (Data of control group and mice treated with 5 MBq and 10 MBq of [^{177}Lu]Lu-SibuDAB were previously published (*27,28*).)

survival, 43.5 d), whereas all mice treated with [^{177}Lu]Lu-PSMA-I&T reached an endpoint by day 41 (median survival, 28 d). When the application was 10 MBq, 4 of 6 mice injected with [^{161}Tb]Tb-PSMA-I&T were alive at study end, whereas only 1 of 6 mice in the group that received [^{177}Lu]Lu-PSMA-I&T was alive at study end (Figs. 4B and 4D).

The therapeutic efficacy was quantitatively expressed as the average of the AUC_{RTV} for mice in each group (Table 1). These values were 1.3-fold and 1.7-fold smaller for mice injected with 2 MBq or 5 MBq, respectively, of [^{161}Tb]Tb-SibuDAB than for mice treated ith equal activities of [^{177}Lu]Lu-SibuDAB. The AUC_{RTV} was 2.4- and 2.2-fold lower for mice that received 5 or 10 MBq of [^{161}Tb]Tb-PSMA-I&T, respectively, than for mice treated with equal activities of [^{177}Lu]Lu-PSMA-I&T.

Analysis of Potential Adverse Events During Therapy

The body mass of mice with effective tumor shrinkage increased over time, with the average body mass of mice treated with 10 MBq of radioligand being in the same range on the day of euthanasia as for untreated, non–tumor-bearing control mice of the same age ($P > 0.05$; Supplemental Fig. 3). In contrast, rapid tumor growth was associated with body mass loss, which was observed for PC-3 PIP tumor–bearing mice that received only vehicle and for mice treated with the lowest activity.

Blood urea nitrogen, albumin, alkaline phosphatase, and total bilirubin in blood plasma were in the same range for mice treated with 10 MBq of radioligands and non–tumor-bearing control mice. The same held true for blood cell counts ($P > 0.05$; Fig. 5; Supplemental Tables 8 and 9). The leukocyte, erythrocyte, and thrombocyte counts were in the reference range irrespective of the applied treatment. Histopathologic analysis of the kidneys, liver, salivary glands, spleen, and bone marrow did not indicate any changes after RLT (Supplemental Table 10).

DISCUSSION

Several preclinical studies demonstrated the superiority of ^{161}Tb over ^{177}Lu (*17,18,30*), which was supported by dose calculations that consistently proposed the benefit of the coemitted conversion and Auger electrons by ^{161}Tb (*15,16,31*). The fact that ^{161}Tb can be produced in large quantities, in analogy to ^{177}Lu (*32*), and the commercial interest of companies to produce ^{161}Tb make this radionuclide particularly attractive for clinical translation.

In agreement with our previous study performed with [^{161}Tb]Tb-PSMA-617 and [^{177}Lu]Lu-PSMA-617 (*18*), the in vitro properties and tissue distribution profiles of [^{161}Tb]Tb-SibuDAB and [^{161}Tb]Tb-PSMA-I&T were similar to their respective ^{177}Lu-labeled counterparts. Dosimetry estimations were thus based on data obtained with [^{177}Lu]Lu-SibuDAB and [^{177}Lu]Lu-PSMA-I&T. Estimation of the radiation dose of [^{161}Tb]Tb-SibuDAB and [^{161}Tb]Tb-PSMA-I&T would most likely be feasible also for clinical data currently being

TABLE 1
Parameters Indicative of Efficacy of Treatment

Treatment	Injected activity (MBq)	First mouse euthanized (d)*	Last mouse euthanized (d)*	Median survival (d)	Mice alive on day 56	AUC_{RTV}
Saline†	—	14	28	18	0/12	477 ± 148
[^{161}Tb]Tb-SibuDAB	2	25	56	32.5	1/6	233 ± 111
[^{177}Lu]Lu-SibuDAB	2	22	56	23	1/6	306 ± 172
[^{161}Tb]Tb-SibuDAB	5	56	56	>>56‡	6/6	29 ± 16
[^{177}Lu]Lu-SibuDAB†	5	49	56	>>56‡	5/6	50 ± 50
[^{161}Tb]Tb-SibuDAB	10	56	56	>>56‡	6/6	20 ± 5
[^{177}Lu]Lu-SibuDAB§	10	56	56	>>56‡	6/6	18 ± 8
[^{161}Tb]Tb-PSMA-I&T	5	24	56	43.5	3/6	147 ± 134
[^{177}Lu]Lu-PSMA-I&T	5	18	41	28	0/6	356 ± 177
[^{161}Tb]Tb-PSMA-I&T	10	48	56	>>56‡	4/6	49 ± 42
[^{177}Lu]Lu-PSMA-I&T	10	28	56	43	2/6	108 ± 81

*All mice that did not reach endpoint were euthanized on day 56.
†Data were previously published (*27*).
‡Exact median survival could not be defined, since more than half of mice survived until study end (day 56).
§Data were previously published (*28*).

acquired for [^{177}Lu]Lu-SibuDAB and already published for [^{177}Lu]Lu-PSMA-I&T (*33*). ^{161}Tb delivers a slightly higher dose to the tissue than ^{177}Lu because of the 15% increased β^--energy (average β^- energy, 154 vs. 134 keV). More importantly, the coemission of conversion and Auger electrons contributes substantially to the enhanced dose of ^{161}Tb depending on the sphere radius assumed for the tumor size (*15*). In the current study, the absorbed tumor dose estimated for the ^{161}Tb-based PSMA ligands was 40% higher than that of the ^{177}Lu-based counterparts. As a result, and in agreement with previous studies using other targeting agents (*17,30*), our data showed consistently enhanced antitumor efficacy and prolonged survival in mice treated with the ^{161}Tb-labeled versions of SibuDAB and PSMA-I&T as compared with mice that received their ^{177}Lu-labeled counterparts.

Because the albumin-binding properties of SibuDAB enhanced tumor uptake considerably, [^{161}Tb]Tb-SibuDAB demonstrated an approximately 4-fold higher absorbed tumor dose than [^{161}Tb]Tb-PSMA-I&T. [^{161}Tb]Tb-SibuDAB, applied at the same activity as [^{161}Tb]Tb-PSMA-I&T, thus showed better therapeutic efficacy as demonstrated by the 2.5- to 5-fold enhanced tumor growth inhibition quantified on the basis of the AUC_{RTV}. According to dosimetry calculations, a complete tumor response could most likely also be achieved with approximately 20 MBq of [^{161}Tb]Tb-PSMA-I&T or approximately 25 MBq of [^{177}Lu]Lu-PSMA-I&T applied under the given experimental conditions.

Since the absorbed kidney dose was similar for both radioligands, [^{161}Tb]Tb-SibuDAB showed a more favorable tumor-to-kidney dose ratio than [^{161}Tb]Tb-PSMA-I&T. Assuming 23 Gy as the kidney dose limit (*34*), 4–5 therapy cycles of 10 MBq of [^{161}Tb]Tb-SibuDAB or [^{161}Tb]Tb-PSMA-I&T could be safely applied; thus, no kidney toxicity was observed in our study. In agreement with other reported preclinical studies (*35*), kidney uptake was considerably higher for [^{161}Tb]Tb/[^{177}Lu]Lu-PSMA-I&T than for [^{161}Tb]Tb/[^{177}Lu]Lu-PSMA-617 tested in the same tumor mouse model (*18*). In patients, renal retention of [^{177}Lu]Lu-PSMA-I&T and [^{177}Lu]Lu-PSMA-617 was more similar (*36*) and radionephrotoxicity was only rarely reported in the literature (*37,38*).

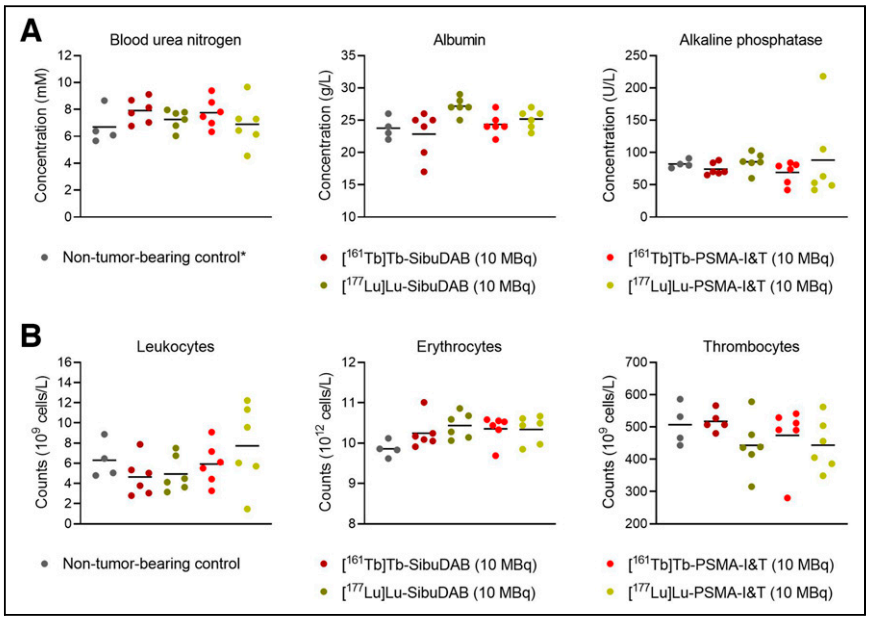

FIGURE 5. (A) Blood plasma parameters: blood urea nitrogen, albumin, and alkaline phosphatase. (B) Blood cell counts of leukocytes, erythrocytes, and thrombocytes. *Data were previously published (*28*).

Regarding other organs and tissues, the applied RLT in our study was well tolerated in mice, irrespective of the ligand and radionuclide applied. It is noteworthy, however, that salivary gland toxicity cannot be investigated in mice and therefore has to be carefully assessed in clinical studies conducted with ^{161}Tb-based RLT.

Because mice seem to be less susceptible to undesired effects of RLT than humans, much higher activities would probably be necessary to observe hematotoxicity (*39,40*). Indeed, previous experiments showed that [^{177}Lu]Lu-(*R/S*)-Ibu-DAB-PSMA (30 MBq per mouse) was well tolerated in immunocompetent mice over the first month after treatment (*26*).

Potential limitations of our study relate to the fact that an extrapolation from mice to men may not be easily feasible and that bone marrow dose calculations can hardly be performed for mice. It is likely, however, that bone marrow represents the dose-limiting organ for application of albumin-binding PSMA radioligands. Investigations of the tissue distribution profile of [^{161}Tb]Tb/[^{177}Lu]Lu-SibuDAB thus remain to be assessed in patients, and the favorable preclinical findings of using ^{161}Tb remain to be confirmed clinically. As the proposed benefit of using ^{161}Tb over ^{177}Lu refers mainly to the elimination of single cancer cells and micrometastases, ^{161}Tb-based radioligands should be tested in a follow-up study using mouse models of metastasized disease.

CONCLUSION

The superior therapeutic efficacy of ^{161}Tb over ^{177}Lu in combination with PSMA ligands agreed with the increased estimated absorbed tumor dose. The data of this study indicate particularly promising potential for [^{161}Tb]Tb-SibuDAB in the RLT of prostate cancer patients. Generally, the clinical translation of ^{161}Tb-based RLT appears promising, yet the therapeutic window for each of these radioligands must be carefully assessed.

DISCLOSURE

Viviane Tschan was funded by an iDoc grant from the Personalized Medicine and Related Technology program (PHRT-301; principal investigator, Cristina Müller). The research was supported by the Swiss Cancer Research Foundation (KFS-4678-02-2019-R; principal investigator, Cristina Müller) and by the Swiss National Science Foundation (310030_188978; principal investigator, Cristina Müller). Peter Bernhardt received grants from the Swedish Cancer Society, the Swedish Research Council, the King Gustav V Jubilee Clinic Cancer Research Foundation, and the Swedish state under the agreement between the Swedish government and the county councils (an ALF agreement). The project was further supported by ITM Isotope Technologies Munich SE, Germany, which delivered free ^{177}Lu for all the performed studies. The following is a competing financial interest: patent applications on albumin-binding PSMA ligands have been filed by ITM Isotope Technologies Munich SE, Germany, in which Roger Schibli and Cristina Müller are listed as coinventors. No other potential conflict of interest relevant to this article was reported.

ACKNOWLEDGMENTS

We thank Luisa M. Deberle, Anna E. Becker, Susan Cohrs, Fan Sozzi-Guo, Colin Hillhouse, and Rebekka Mayer for technical assistance with the experiments at Paul Scherrer Institute, Switzerland.

KEY POINTS

QUESTIONS: How effective is the therapeutic application of ^{161}Tb in combination with albumin-binding and conventional PSMA ligands in comparison to their respective ^{177}Lu-labeled analogs?

PERTINENT FINDINGS: These preclinical therapy studies confirmed the benefit of ^{161}Tb-based RLT over ^{177}Lu-based RLT in PSMA-positive tumor-bearing mice. It was also shown that [^{161}Tb]Tb-SibuDAB was more powerful than [^{161}Tb]Tb-PSMA-I&T because of its increased tumor uptake and, hence, absorbed tumor dose.

IMPLICATIONS FOR PATIENT CARE: These preclinical data set the basis for future clinical translation of ^{161}Tb-based RLT using albumin-binding and conventional PSMA radioligands.

REFERENCES

1. Kulkarni HR, Singh A, Schuchardt C, et al. PSMA-based radioligand therapy for metastatic castration-resistant prostate cancer: the Bad Berka experience since 2013. *J Nucl Med.* 2016;57(suppl 3):97S–104S.
2. Rahbar K, Ahmadzadehfar H, Kratochwil C, et al. German multicenter study investigating ^{177}Lu-PSMA-617 radioligand therapy in advanced prostate cancer patients. *J Nucl Med.* 2017;58:85–90.
3. Violet J, Sandhu S, Iravani A, et al. Long-term follow-up and outcomes of retreatment in an expanded 50-patient single-center phase II prospective trial of ^{177}Lu-PSMA-617 theranostics in metastatic castration-resistant prostate cancer. *J Nucl Med.* 2020;61:857–865.
4. Sartor O, de Bono J, Chi KN, et al. Lutetium-177-PSMA-617 for metastatic castration-resistant prostate cancer. *N Engl J Med.* 2021;385:1091–1103.
5. Weineisen M, Schottelius M, Simecek J, et al. ^{68}Ga- and ^{177}Lu-labeled PSMA I&T: optimization of a PSMA-targeted theranostic concept and first proof-of-concept human studies. *J Nucl Med.* 2015;56:1169–1176.
6. Chatalic KL, Heskamp S, Konijnenberg M, et al. Towards personalized treatment of prostate cancer: PSMA I&T, a promising prostate-specific membrane antigen-targeted theranostic agent. *Theranostics.* 2016;6:849–861.
7. Heck MM, Tauber R, Schwaiger S, et al. Treatment outcome, toxicity, and predictive factors for radioligand therapy with ^{177}Lu-PSMA-I&T in metastatic castration-resistant prostate cancer. *Eur Urol.* 2019;75:920–926.
8. Privé BM, Janssen MJR, van Oort IM, et al. Update to a randomized controlled trial of lutetium-177-PSMA in oligo-metastatic hormone-sensitive prostate cancer: the BULLSEYE trial. *Trials.* 2021;22:768.
9. Azad A, Dhiantravan N, Emmett L, et al. UpFrontPSMA: a randomized phase II study of sequential ^{177}Lu-PSMA617 and docetaxel versus docetaxel in metastatic hormone-naïve prostate cancer (mHNPC) [abstract]. *J Clin Oncol.* 2021;39(suppl): TPS180.
10. Alghazo O, Eapen R, Dhiantravan N, et al. Study of the dosimetry, safety, and potential benefit of ^{177}Lu-PSMA-617 radionuclide therapy prior to radical prostatectomy in men with high-risk localized prostate cancer (LuTectomy study) [abstract]. *J Clin Oncol.* 2021;39(suppl):TPS264.
11. Sartor AO, Tagawa ST, Saad F, et al. PSMAddition: a phase 3 trial to compare treatment with ^{177}Lu-PSMA-617 plus standard of care (SOC) versus SOC alone in patients with metastatic hormone-sensitive prostate cancer [abstract]. *J Clin Oncol.* 2022;40(suppl):TPS210.
12. Golan S, Frumer M, Zohar Y, et al. Neoadjuvant ^{177}Lu-PSMA-I&T radionuclide treatment in patients with high-risk prostate cancer before radical prostatectomy: a single-arm phase 1 trial. *Eur Urol Oncol.* 2023;6:151–159.
13. Feuerecker B, Tauber R, Knorr K, et al. Activity and adverse events of actinium-225-PSMA-617 in advanced metastatic castration-resistant prostate cancer after failure of lutetium-177-PSMA. *Eur Urol.* 2021;79:343–350.
14. Lee DY, Kim YI. Effects of ^{225}Ac-labeled prostate-specific membrane antigen radioligand therapy in metastatic castration-resistant prostate cancer: a meta-analysis. *J Nucl Med.* 2022;63:840–846.
15. Hindié E, Zanotti-Fregonara P, Quinto MA, Morgat C, Champion C. Dose deposits from ^{90}Y, ^{177}Lu, ^{111}In, and ^{161}Tb in micrometastases of various sizes: implications for radiopharmaceutical therapy. *J Nucl Med.* 2016;57:759–764.
16. Alcocer-Avila ME, Ferreira A, Quinto MA, Morgat C, Hindie E, Champion C. Radiation doses from ^{161}Tb and ^{177}Lu in single tumour cells and micrometastases. *EJNMMI Phys.* 2020;7:33.

17. Müller C, Reber J, Haller S, et al. Direct in vitro and in vivo comparison of ^{161}Tb and ^{177}Lu using a tumour-targeting folate conjugate. *Eur J Nucl Med Mol Imaging.* 2014;41:476–485.
18. Müller C, Umbricht CA, Gracheva N, et al. Terbium-161 for PSMA-targeted radionuclide therapy of prostate cancer. *Eur J Nucl Med Mol Imaging.* 2019;46: 1919–1930.
19. Borgna F, Barritt P, Grundler PV, et al. Simultaneous visualization of ^{161}Tb- and ^{177}Lu-labeled somatostatin analogues using dual-isotope SPECT imaging. *Pharmaceutics.* 2021;13:536.
20. Buteau JP, Kostos LK, Alipour R, et al. VIOLET: a phase I/II trial evaluation of radioligand treatment in men with metastatic castration-resistant prostate cancer with [^{161}Tb]Tb-PSMA-I&T [abstract]. *J Clin Oncol.* 2023;41(suppl):TPS281.
21. Rosar F, Maus S, Schaefer-Schuler A, Burgard C, Khreish F, Ezziddin S. New horizons in radioligand therapy: ^{161}Tb-PSMA-617 in advanced mCRPC. *Clin Nucl Med.* 2023;48:433–434.
22. Al-Ibraheem A, Doudeen RM, Juaidi D, Abufara A, Maus S. ^{161}Tb-PSMA radioligand therapy: first-in-human SPECT/CT imaging. *J Nucl Med.* February 9, 2023 [Epub ahead of print].
23. Umbricht CA, Benesova M, Schibli R, Müller C. Preclinical development of novel PSMA-targeting radioligands: modulation of albumin-binding properties to improve prostate cancer therapy. *Mol Pharm.* 2018;15:2297–2306.
24. Kramer V, Fernandez R, Lehnert W, et al. Biodistribution and dosimetry of a single dose of albumin-binding ligand [^{177}Lu]Lu-PSMA-ALB-56 in patients with mCRPC. *Eur J Nucl Med Mol Imaging.* 2021;48:893–903.
25. Deberle LM, Benesova M, Umbricht CA, et al. Development of a new class of PSMA radioligands comprising ibuprofen as an albumin-binding entity. *Theranostics.* 2020;10:1678–1693.
26. Tschan VJ, Borgna F, Busslinger SD, et al. Preclinical investigations using [^{177}Lu]Lu-Ibu-DAB-PSMA toward its clinical translation for radioligand therapy of prostate cancer. *Eur J Nucl Med Mol Imaging.* 2022;49:3639–3650.
27. Borgna F, Deberle LM, Busslinger SD, et al. Preclinical investigations to explore the difference between the diastereomers [^{177}Lu]Lu-SibuDAB and [^{177}Lu]Lu-RibuDAB toward prostate cancer therapy. *Mol Pharm.* 2022;19:2105–2114.
28. Busslinger SD, Tschan VJ, Richard OK, Talip Z, Schibli R, Müller C. [^{225}Ac]Ac-SibuDAB for targeted alpha therapy of prostate cancer: preclinical evaluation and comparison with [^{225}Ac]Ac-PSMA-617. *Cancers (Basel).* 2022;14:5651.
29. Salvat F. *PENELOPE-2014: A Code System for Monte Carlo Simulation of Electron and Photon Transport.* OECD; 2015:1–386.
30. Borgna F, Haller S, Rodriguez JMM, et al. Combination of terbium-161 with somatostatin receptor antagonists: a potential paradigm shift for the treatment of neuroendocrine neoplasms. *Eur J Nucl Med Mol Imaging.* 2022;49:1113–1126.
31. Bernhardt P, Svensson J, Hemmingsson J, et al. Dosimetric analysis of the short-ranged particle emitter ^{161}Tb for radionuclide therapy of metastatic prostate cancer. *Cancers (Basel).* 2021;13:2011.
32. Gracheva N, Müller C, Talip Z, et al. Production and characterization of no-carrier-added ^{161}Tb as an alternative to the clinically-applied ^{177}Lu for radionuclide therapy. *EJNMMI Radiopharm Chem.* 2019;4:12.
33. Okamoto S, Thieme A, Allmann J, et al. Radiation dosimetry for ^{177}Lu-PSMA I&T in metastatic castration-resistant prostate cancer: absorbed dose in normal organs and tumor lesions. *J Nucl Med.* 2017;58:445–450.
34. Haller S, Reber J, Brandt S, et al. Folate receptor-targeted radionuclide therapy: preclinical investigation of anti-tumor effects and potential radionephropathy. *Nucl Med Biol.* 2015;42:770–779.
35. Ruigrok EAM, van Vliet N, Dalm SU, et al. Extensive preclinical evaluation of lutetium-177-labeled PSMA-specific tracers for prostate cancer radionuclide therapy. *Eur J Nucl Med Mol Imaging.* 2021;48:1339–1350.
36. Schuchardt C, Zhang J, Kulkarni HR, Chen X, Muller D, Baum RP. Prostate-specific membrane antigen radioligand therapy using ^{177}Lu-PSMA I&T and ^{177}Lu-PSMA-617 in patients with metastatic castration-resistant prostate cancer: comparison of safety, biodistribution, and dosimetry. *J Nucl Med.* 2022;63:1199–1207.
37. Hartrampf PE, Weinzierl FX, Serfling SE, et al. Hematotoxicity and nephrotoxicity in prostate cancer patients undergoing radioligand therapy with [^{177}Lu]Lu-PSMA I&T. *Cancers (Basel).* 2022;14:647.
38. Hartrampf PE, Weinzierl FX, Buck AK, et al. Matched-pair analysis of [^{177}Lu]Lu-PSMA I&T and [^{177}Lu]Lu-PSMA-617 in patients with metastatic castration-resistant prostate cancer. *Eur J Nucl Med Mol Imaging.* 2022;49:3269–3276.
39. Fendler WP, Stuparu AD, Evans-Axelsson S, et al. Establishing ^{177}Lu-PSMA-617 radioligand therapy in a syngeneic model of murine prostate cancer. *J Nucl Med.* 2017;58:1786–1792.
40. Kristiansson A, Vilhelmsson Timmermand O, Altai M, et al. Hematological toxicity in mice after high activity injections of ^{177}Lu-PSMA-617. *Pharmaceutics.* 2022;14:731.